# ERROR ESTIMATES FOR EULER DISCRETIZATION OF HIGH-INDEX SADDLE DYNAMICS[*]

LEI ZHANG[†], PINGWEN ZHANG[‡], AND XIANGCHENG ZHENG[§]

**Abstract.** High-index saddle dynamics provide an effective means to compute the any-index saddle points and construct the solution landscape. In this paper, we prove error estimates for Euler discretization of high-index saddle dynamics with respect to the time step size, which remains untreated in the literature. We overcome the main difficulties that lie in the strong nonlinearity of the saddle dynamics and the orthonormalization procedure in the numerical scheme that is uncommon in standard discretization of differential equations. The derived methods are further extended to study the generalized high-index saddle dynamics for nongradient systems and provide theoretical support for the accuracy of numerical implementations.

**Key words.** saddle point, saddle dynamics, solution landscape, Euler scheme, error estimate

**MSC codes.** 37M05, 37N30, 65L20

**DOI.** 10.1137/21M1458314

**1. Introduction.** Finding stationary points of nonlinear multivariable energy functions $E(x)$ has attracted extensive interest in different scientific communities during the past few decades. It plays a crucial role in determining many physical or chemical properties of complex systems, examples of which include the critical nuclei in phase transition [5, 37, 34, 35], defects in liquid crystals [11, 24], self-assembly of polymers [12, 25], molecular clusters [1, 3], and artificial neural networks [9]. According to Morse theory [21], the local stability of stationary points, including both stable minima and unstable saddle points, can be characterized by the Morse index. The (Morse) index of a nondegenerate saddle point is the maximal dimension of a subspace on which its Hessian matrix is negative definite, i.e., the number of negative eigenvalues of the Hessian matrix. In particular, the stable stationary point (minimizer) can be regarded as an index-0 saddle point with no unstable direction.

Due to the complex geometric structures of the energy functions and the unstable nature of saddle points, how to efficiently compute multiple stationary points remains a challenging problem [3, 7, 18, 20]. Most existing efforts focus on finding the index-1 saddle point or transition state, i.e., a stationary point where the Hessian has one and only one negative eigenvalue. One of the popular approaches is the class of surface walking methods [37]. In particular, the dimer-type method [15, 33, 36] and the gentlest ascent dynamics [6], as the representatives of the surface walking methods, were developed to compute the index-1 saddle points. Recently, inspired by

[†]Beijing International Center for Mathematical Research, Center for Quantitative Biology, Center for Machine Learning Research, Peking University, Beijing 100871, China (zhangl@math.pku.edu.cn).

[‡]School of Mathematical Sciences, Laboratory of Mathematics and Applied Mathematics, Peking University, Beijing 100871, China (pzhang@pku.edu.cn).

[§]School of Mathematical Sciences, Peking University, Beijing 100871, China (zhengxch@math.pku.edu.cn).

the optimization-based shrinking dimer method [36], the high-index saddle dynamics (HiSD) were proposed to search for any-index saddle points [31]. The HiSD method provides an efficient tool to construct the solution landscape of the energy systems, which describes a pathway map that starts with a parent state (the highest-index saddle point) and then relates the low-index saddle points down to all the minimizers [29]. The solution landscape approach has been applied to study various physical systems such as liquid crystals [14, 13, 32], polymers [26], and quasicrystals [28]. Moreover, based on the HiSD method, generalized high-index saddle dynamics (GHiSD) were further proposed to compute the any-index saddle points and solution landscapes of dynamical (nongradient) systems [30].

Despite the sustained development of the saddle-point searching algorithms, the rigorous numerical analysis on them is still far from well developed. Some existing studies mainly focus on the index-1 saddle points. For instance, in [33], the time discretization of the shrinking dimer dynamics was studied, and the linear local asymptotic stability analysis and optimal error reduction rates were carried out. Global convergence and nonlinear asymptotic stability were also illustrated for some specific systems. In [10], the dimer method with linesearch for the step size and the preconditioning was investigated. Local convergence and error reduction were proved and, in particular, the $O(l^2)$ accuracy between the stationary point of the algorithm and the saddle was proved where $l$ refers to the dimer length. In [16], the existing local convergence results for dimer-type and gentlest ascent dynamics methods were extended by developing an improved estimate on the region of attraction of index-1 saddle points that goes beyond the linearized regime. In [8], a quadratic local convergence rate in terms of the number of iterations was proved for an iterative minimization scheme for searching index-1 saddle points of energy functions.

The aforementioned works, which provide asymptotic convergence results of, e.g., $x_n - x_*$, where $x_n$ and $x_*$ refer to the numerical solution at the $n$th iteration and the limit (target saddle point) of the scheme, respectively, made significant progress on the theoretical foundation of numerical analysis of the saddle-point searching algorithms. In contrast, the error estimate of $x_n - x(t_n)$, where $x(t_n)$ represents the exact solution of HiSD at the step $t_n$, gives the dynamical pathway convergence of numerical solutions to the saddle dynamics, which provides important physical information, such as the transition pathway [28], and theoretically ensures the accuracy of the constructed solution landscape [29]. Inaccurate computations of the dynamical pathway could lead to missing saddle points and an incomplete solution landscape. Therefore, it is necessary and meaningful to perform the error estimates of $x_n - x(t_n)$ for HiSD, which motivates the investigations in the work. Furthermore, the existing numerical analysis only focuses on the schemes of finding index-1 saddle points, while the corresponding results for numerical methods of finding high-index saddle points in [30, 31] are still unavailable.

Motivated by these discussions, in this paper we aim to prove error estimates for the Euler discretization of the HiSD method with respect to the time step size, which focuses more on the dynamics (i.e., the searching pathways between saddle points) than its limit. We emphasize that there exist some essential differences and challenges from the standard methods of ODEs. First, the rigorous numerical analysis on saddle-point searching algorithms is more challenging than gradient descent methods for finding the minima, which remains untreated for the high-index saddle points in particular. For instance, in (4.3) the left-hand side of the scheme of the $i$th eigenvector $v_i$ is not its numerical approximation $v_{i,n}$ at the step $t_n$, but an intermediate quantity $\tilde{v}_{i,n}$. This is due to the fact that the outcomes $\{\tilde{v}_{i,n}\}$ of the schemes of $\{v_i\}$ may not

be orthonormal and thus need to be further processed in the third equation of (4.3). Consequently, in order to generate the error equations by subtracting the schemes from the reference equations, we will encounter $v_i(t_n) - \tilde{v}_{i,n}$ instead of $v_i(t_n) - v_{i,n}$ as in the case of ODE discretizations. A natural idea is to split $v_i(t_n) - \tilde{v}_{i,n}$ as $(v_i(t_n) - v_{i,n}) + (v_{i,n} - \tilde{v}_{i,n})$, which requires an additional estimate of $v_{i,n} - \tilde{v}_{i,n}$ that is not common in numerical methods of ODEs. Since $\{v_{i,n}\}$ is generated from $\{\tilde{v}_{i,n}\}$ via the orthonormalization, careful estimates are required for this procedure, which is intricate and not available in the literature. Furthermore, to support this analysis, novel techniques are developed to overcome the strong nonlinearity of the HiSD to prove several properties of the numerical solutions based on their schemes, which serves as another highlight. The aforementioned issues are the main contributions of the current work and distinguish the proposed methods from the standard numerical analysis of ODEs. By subtle treatments and estimates, we rigorously prove the first-order accuracy of the numerical scheme, which contributes to the numerical theory of HiSD and provides theoretical support for the accuracy of numerical computations.

The rest of this paper is organized as follows: In section 2 we present formulations of HiSD. In section 3 we prove the error estimates for Euler discretization of index-1 saddle dynamics. In section 4 we extend the developed techniques to prove error estimates for the Euler discretization of index-$k$ saddle dynamics. Numerical experiments are performed in section 5 to substantiate the theoretical findings. In section 6 we extend the proposed techniques to study the GHiSD of nongradient systems, and we finally address the concluding remarks in section 7.

**2. Formulation of HiSD.** Given a twice Fréchet differentiable energy functional $E(x)$ with $x \in \mathbb{R}^N$, we define the corresponding natural force $F : \mathbb{R}^N \to \mathbb{R}^N$ and the negative Hessian $J \in \mathbb{R}^{N \times N}$ by $F(x) = -\nabla E(x)$ and $J(x) = -\nabla^2 E(x)$. It is clear that $J(x) = J(x)^\top$. Then the saddle dynamics for an index-$k$ saddle point ($k$-SD) of $E(x)$ with $1 \le k \in \mathbb{N}$ reads [31]

$$(2.1) \quad \begin{cases} \dfrac{dx}{dt} = \beta\left(I - 2\sum_{j=1}^{k} v_j v_j^\top\right)F(x), \\ \dfrac{dv_i}{dt} = \gamma\left(I - v_i v_i^\top - 2\sum_{j=1}^{i-1} v_j v_j^\top\right)J(x)v_i, \quad 1 \le i \le k, \end{cases}$$

where $x$ represents a position variable, $v_i(i = 1, \ldots, k)$ are $k$ directional variables, and $\beta, \gamma > 0$ are relaxation parameters. The system (2.1) was formulated by the minimax optimization framework, and it was shown in [31, Theorem 1] that, under suitable assumptions, a linearly stable solution of (2.1) is an index-$k$ saddle point of $E(x)$ associated with $k$ eigenvectors corresponding to the $k$ negative eigenvalues of its Hessian. Furthermore, it is shown in [31] that if the initial values of $\{v_i(t)\}_{i=1}^{k}$ for (2.1) are orthonormal vectors, then

$$(2.2) \quad \|v_i(t)\| = 1, \quad 1 \le i \le k \quad \forall t > 0.$$

In particular, the index-1 saddle points attract much interest as they connect different minimizers. This corresponds to the simplest case of (2.1) with $k = 1$, i.e., 1-SD, which is also equivalent to the gentlest ascent dynamics proposed in [6],

$$(2.3) \quad \begin{cases} \dfrac{dx}{dt} = \beta(I - 2vv^\top)F(x), \\ \dfrac{dv}{dt} = \gamma(I - vv^\top)J(x)v. \end{cases}$$

Throughout this paper we make the following regular assumptions on the force and the Hessian.

**Assumption A.** There exists a constant $L > 0$ such that the following linear growth and Lipschitz conditions hold under the standard $l^2$ norm $\| \cdot \|$ of a vector or a matrix:

$$\|J(x_2) - J(x_1)\| + \|F(x_2) - F(x_1)\| \leq L\|x_2 - x_1\|,$$

$$\|F(x)\| \leq L(1 + \|x\|), \quad x, x_1, x_2 \in \mathbb{R}^N.$$

*Remark* 2.1. In many applications, there exist various energy functions $E$ satisfying Assumption A, such as the Minyaev–Quapp surface [22]

$$(2.4) \qquad E(x_1, x_2) = \cos(2x_1) + \cos(2x_2) + 0.57\cos(2x_1 - 2x_2)$$

and the Eckhardt surface [4]

$$(2.5) \qquad \begin{aligned} E(x_1, x_2) &= \exp(-x_1^2 - (x_2 + 1)^2) \\ &\quad + \exp(-x_1^2 - (x_2 - 1)^2) + 4\exp\left(-3\frac{x_1^2 + x_2^2}{2}\right) + \frac{x_2^2}{2}. \end{aligned}$$

We then cite the continuous and discrete Gronwall inequalities that will be frequently used in this paper [2].

LEMMA 2.1. *Assume $z$, $g$, and $k$ are continuous functions on $[0, T]$, $z \geq 0$, $k \geq 0$, $g$ is nondecreasing, and*

$$z(t) \leq g(t) + \int_0^t k(s)z(s)ds, \quad t \in [0, T].$$

*Then the following estimate holds:*

$$z(t) \leq g(t)\exp\left(\int_0^t k(s)ds\right), \quad t \in [0, T].$$

*Assume that the nonnegative sequences $\{z_n\}_{n\geq 1}$ and $\{k_n\}_{n\geq 1}$ satisfy*

$$z_n \leq \rho + \sum_{j=1}^{n-1} k_j z_j, \quad n \geq 1$$

*for some $\rho \geq 0$. Then the following estimate holds:*

$$z_n \leq \rho\exp\left(\sum_{j=1}^{n-1} k_j\right), \quad n \geq 1.$$

By (2.2), we multiply the first equation in (2.1) by $x^\top$ to obtain

$$(2.6) \qquad \begin{aligned} \frac{1}{2}\frac{d}{dt}\|x\|^2 = x^\top \frac{dx}{dt} &= \beta x^\top F(x) - 2\beta \sum_{j=1}^{k} v_j^\top F(x)x^\top v_j \\ &\leq \beta\|x\|\|F(x)\| + 2\beta k\|x\|\|F(x)\| \\ &\leq (1 + 2k)\beta L\|x\|(1 + \|x\|) \\ &\leq \frac{3(1 + 2k)\beta L}{2}\|x\|^2 + \frac{(1 + 2k)\beta L}{2}, \end{aligned}$$

which leads to

$$(2.7) \qquad \|x(t)\|^2 \leq \|x(0)\|^2 + 3(1+2k)\beta L \int_0^t \|x(s)\|^2 ds + (1+2k)\beta Lt.$$

Then for a terminal time $T > 0$, an application of the Gronwall inequality in Lemma 2.1 yields

$$(2.8) \qquad \|x\|^2 \leq \big(\|x(0)\|^2 + (1+2k)\beta LT\big)e^{3(1+2k)\beta LT} =: Q_T.$$

That is, within any terminal time $T$, $\|x\|$ can be bounded by some fixed constant $\sqrt{Q_T}$, and we thus assume

$$J_T := \max_{\|x\| \leq \sqrt{Q_T}} \|J(x)\|.$$

**3. Numerical analysis for index-1 saddle dynamics.** In this section, we consider the explicit Euler scheme of 1-saddle dynamics (1-SD) (2.3) on the time interval $[0, T]$ for some $T > 0$ equipped with the initial conditions

$$(3.1) \qquad x(0) = x_0, \quad v(0) = v_0, \quad \|v_0\|_2 = 1.$$

Although this is mathematically a special case of $k$-SD (2.1), it is indeed the most-considered case and could elucidate some key ideas of the analysis in a clear manner.

**3.1. Explicit Euler scheme.** For $N_T \in \mathbb{N}$, we define a uniform temporal partition of $[0, T]$ by $t_n = n\tau$ for $0 \leq n \leq N_T$, where $\tau = T/N_T$ stands for the time step size. We then approximate the first-order derivative by the backward Euler scheme at $t_n$ as follows:

$$\frac{dg(t_n)}{dt} = \frac{g(t_n) - g(t_{n-1})}{\tau} + R_n^g,$$

where $g$ refers to $x$ or $v$, and the truncation error $\|R_n^g\| = O(\tau)$. Plugging this discretization into (2.3) yields

$$(3.2) \quad \begin{cases} x(t_n) = x(t_{n-1}) + \tau\beta\big(I - 2v(t_{n-1})v(t_{n-1})^\top\big)F(x(t_{n-1})) + \tau R_n^x, \\ v(t_n) = v(t_{n-1}) + \tau\gamma\big(I - v(t_{n-1})v(t_{n-1})^\top\big)J(x(t_{n-1}))v(t_{n-1}) + \tau R_n^v. \end{cases}$$

Then we drop the truncation errors to obtain the explicit Euler scheme of (2.3) with the approximations $\{x_n, v_n\}_{n=1}^{N_T}$ to $\{x(t_n), v(t_n)\}_{n=1}^{N_T}$,

$$(3.3) \quad \begin{cases} x_n = x_{n-1} + \tau\beta\big(I - 2v_{n-1}v_{n-1}^\top\big)F(x_{n-1}), \\ \tilde{v}_n = v_{n-1} + \tau\gamma\big(I - v_{n-1}v_{n-1}^\top\big)J(x_{n-1})v_{n-1}, \\ v_n = \dfrac{\tilde{v}_n}{\|\tilde{v}_n\|} \end{cases}$$

for $1 \leq n \leq N_T$, equipped with the initial conditions (3.1).

From (3.3) we find that although $\tilde{v}_n$ may not have the unit $l_2$ norm due to the discretization errors, the normalization procedure in the third equation of (3.3) ensures $\|v_n\| = 1$ in order to preserve the unit length of $v$ as in the continuous problem (2.3). We thus multiply $x_n^\top$ on both sides of the first equation of (3.3) to obtain

$$\|x_n\|^2 \leq \|x_n\|\|x_{n-1}\| + \tau\beta\|x_n\|\|F(x_{n-1})\| + \tau\beta\|x_n\|\|F(x_{n-1})\|,$$

which leads to

$$\|x_n\| - \|x_{n-1}\| \leq \tau\beta\|F(x_{n-1})\| + 2\tau\beta\|F(x_{n-1})\| \leq 3\tau\beta L(1 + \|x_{n-1}\|).$$

Summing up this equation from $n = 1$ to $n^* \leq N_T$ yields

$$\|x_{n^*}\| - \|x_0\| \leq 3\beta LT + 3\tau\beta L \sum_{n=1}^{n^*} \|x_{n-1}\|.$$

Then we apply the discrete Gronwall inequality to conclude that there exists a constant $\bar{Q}_T$ like (2.8) such that $\|x_n\| \leq \sqrt{\bar{Q}_T}$ for $0 \leq n \leq N_T$, and we thus assume

$$(3.4) \qquad \bar{J}_T := \max_{\|x\| \leq \sqrt{\bar{Q}_T}} \|J(x)\|.$$

**3.2. Auxiliary estimate of $\tilde{v}_n - v_n$.** If we intend to find the error equation of $e_n^v := v(t_n) - v_n$ by subtracting the second equation of (3.2) from that of (3.3), the right-hand side of the resulting equation has $e_{n-1}^v$ while the left-hand side is $v(t_n) - \tilde{v}_n$ instead of $e_n^v$ due to the normalization, which is uncommon in the context of discretizing differential equations that naturally yields the errors of different time steps on both sides of the error equations. A potential idea to circumvent this issue is to split $v(t_n) - \tilde{v}_n$ as $(v(t_n) - v_n) + (v_n - \tilde{v}_n) = e_n^v + (v_n - \tilde{v}_n)$, which introduces an additional error $v_n - \tilde{v}_n$. In particular, we need to show that the difference $v_n - \tilde{v}_n$ has the magnitude of $O(\tau^2)$ in order to preserve the $O(\tau)$ accuracy of the numerical scheme (3.3), which motivates the following estimate.

LEMMA 3.1. *Under Assumption* A, *the following estimate holds:*

$$\left|\|\tilde{v}_n\| - 1\right| \leq \left|\|\tilde{v}_n\|^2 - 1\right| \leq \tau^2\gamma^2\bar{J}_T^2, \quad 1 \leq n \leq N_T.$$

*Proof.* By $\|v_{n-1}\| = 1$ we multiply $v_{n-1}^\top$ on both sides of the second equation of (3.3) to obtain

$$(3.5) \qquad \begin{aligned} v_{n-1}^\top \tilde{v}_n &= v_{n-1}^\top v_{n-1} \\ &+ \tau\gamma\big(v_{n-1}^\top J(x_{n-1})v_{n-1} - v_{n-1}^\top v_{n-1}v_{n-1}^\top J(x_{n-1})v_{n-1}\big) = 1. \end{aligned}$$

We then multiply $\tilde{v}_n^\top$ on both sides of the second equation of (3.3) and apply (3.5) to obtain

$$(3.6) \qquad \begin{aligned} \|\tilde{v}_n\|^2 &= \tilde{v}_n^\top \tilde{v}_n \\ &= \tilde{v}_n^\top v_{n-1} + \tau\gamma\big(\tilde{v}_n^\top J(x_{n-1})v_{n-1} - \tilde{v}_n^\top v_{n-1}v_{n-1}^\top J(x_{n-1})v_{n-1}\big) \\ &= 1 + \tau\gamma\big(\tilde{v}_n^\top J(x_{n-1})v_{n-1} - v_{n-1}^\top J(x_{n-1})v_{n-1}\big) \\ &= 1 + \tau\gamma\big(\tilde{v}_n - v_{n-1}\big)^\top J(x_{n-1})v_{n-1}. \end{aligned}$$

Subtracting (3.5) from (3.6) we get

$$(3.7) \qquad \big(\tilde{v}_n - v_{n-1}\big)^\top \tilde{v}_n = \tau\gamma\big(\tilde{v}_n - v_{n-1}\big)^\top J(x_{n-1})v_{n-1}.$$

By $\|v_{n-1}\| = 1$ and (3.5) we have

$$\big(\tilde{v}_n - v_{n-1}\big)^\top v_{n-1} = \tilde{v}_n^\top v_{n-1} - v_{n-1}^\top v_{n-1} = 1 - 1 = 0,$$

and we apply this equality and (3.7) to obtain

$$
\begin{aligned}
\|\tilde{v}_n - v_{n-1}\|^2 &= (\tilde{v}_n - v_{n-1})^\top (\tilde{v}_n - v_{n-1}) \\
&= (\tilde{v}_n - v_{n-1})^\top \tilde{v}_n = \tau\gamma\big(\tilde{v}_n - v_{n-1}\big)^\top J(x_{n-1})v_{n-1} \\
&\leq \tau\gamma\|\tilde{v}_n - v_{n-1}\|\|J(x_{n-1})\|\|v_{n-1}\| \\
&\leq \tau\gamma\bar{J}_T\|\tilde{v}_n - v_{n-1}\|,
\end{aligned}
$$

that is,

(3.8)
$$
\|\tilde{v}_n - v_{n-1}\| \leq \tau\gamma\bar{J}_T.
$$

Note that (3.6) implies

(3.9)
$$
\|\tilde{v}_n\|^2 - 1 = \tau\gamma\big(\tilde{v}_n - v_{n-1}\big)^\top J(x_{n-1})v_{n-1}.
$$

We invoke (3.8) in (3.9) to obtain

(3.10)
$$
\big|\|\tilde{v}_n\|^2 - 1\big| \leq \tau\gamma\|\tilde{v}_n - v_{n-1}\|\|J(x_{n-1})\|\|v_{n-1}\| \leq \tau^2\gamma^2\bar{J}_T^2.
$$

We incorporate this estimate with

(3.11)
$$
\big|\|\tilde{v}_n\|^2 - 1\big| = \big(\|\tilde{v}_n\| + 1\big)\big|\|\tilde{v}_n\| - 1\big| \geq \big|\|\tilde{v}_n\| - 1\big|
$$

to complete the proof. □

COROLLARY 3.2. *Under Assumption* A, *the following estimate holds:*

$$
\|\tilde{v}_n - v_n\| \leq \tau^2\gamma^2\bar{J}_T^2, \quad 1 \leq n \leq N_T.
$$

*Proof.* We subtract $\tilde{v}_n$ from $v_n$ to find

$$
\tilde{v}_n - v_n = \tilde{v}_n - \frac{\tilde{v}_n}{\|\tilde{v}_n\|} = \frac{\tilde{v}_n}{\|\tilde{v}_n\|}\big(\|\tilde{v}_n\| - 1\big).
$$

Thus we apply Lemma 3.1 to immediately obtain

$$
\|\tilde{v}_n - v_n\| = \frac{\|\tilde{v}_n\|}{\|\tilde{v}_n\|}\big|\|\tilde{v}_n\| - 1\big| \leq \tau^2\gamma^2\bar{J}_T^2,
$$

which completes the proof. □

**3.3. Error estimates.** Define the errors by

$$
e_n^x := x(t_n) - x_n, \quad e_n^v := v(t_n) - v_n, \quad 1 \leq n \leq N_T.
$$

We first bound $e_n^x$ in terms of $e_n^v$ in the following theorem.

THEOREM 3.3. *Suppose Assumption* A *holds. Then the following estimate holds:*

$$
\|e_n^x\| \leq Q\tau\sum_{m=1}^{n-1}\|e_m^v\| + Q\tau, \quad 1 \leq n \leq N_T.
$$

*Here $Q$ depends on $L$, $T$, and $\beta$ but is independent of $\tau$, $n$, and $N_T$.*

*Proof.* We subtract the first equation of (3.2) from that of (3.3) to obtain

$$
\begin{aligned}
e_n^x = {}& e_{n-1}^x + \tau\beta(F(x(t_{n-1})) - F(x_{n-1})) \\
& -2\tau\beta\big[v(t_{n-1})v(t_{n-1})^\top F(x(t_{n-1})) \\
& \quad -v_{n-1}v_{n-1}^\top F(x_{n-1})\big] + \tau R_n^x \\
= {}& e_{n-1}^x + \tau\beta(F(x(t_{n-1})) - F(x_{n-1})) \\
& -2\tau\beta\big[e_{n-1}^v v(t_{n-1})^\top F(x(t_{n-1})) \\
& \quad +v_{n-1}(e_{n-1}^v)^\top F(x(t_{n-1})) \\
& \quad +v_{n-1}v_{n-1}^\top\big(F(x(t_{n-1})) - F(x_{n-1})\big)\big] + \tau R_n^x.
\end{aligned}
$$
(3.12)

We then apply Assumption A to find

$$
\begin{aligned}
\|e_n^x\| \le {}& \|e_{n-1}^x\| + \tau\beta\|F(x(t_{n-1})) - F(x_{n-1})\| \\
& + 2\tau\beta\big[\|e_{n-1}^v\|\|v(t_{n-1})\|\|F(x(t_{n-1}))\| \\
& \quad + \|v_{n-1}\|\|e_{n-1}^v\|\|F(x(t_{n-1}))\| \\
& \quad + \|v_{n-1}\|\|v_{n-1}\|\|F(x(t_{n-1})) - F(x_{n-1})\|\big] + \tau\|R_n^x\| \\
\le {}& \|e_{n-1}^x\| + \tau\beta L\|e_{n-1}^x\| + 2\tau\beta\big[\|e_{n-1}^v\|L(1 + \sqrt{Q_T}) \\
& \quad + \|e_{n-1}^v\|L(1 + \sqrt{Q_T}) + L\|e_{n-1}^x\|\big] + \tau\|R_n^x\| \\
\le {}& (1 + 3\tau\beta L)\|e_{n-1}^x\| + 4\tau\beta L(1 + \sqrt{Q_T})\|e_{n-1}^v\| + \tau\|R_n^x\|.
\end{aligned}
$$
(3.13)

Adding this equation from $n = 1$ to $n_*$ leads to

$$
\|e_{n_*}^x\| \le 3\tau\beta L \sum_{n=1}^{n_*} \|e_{n-1}^x\| + \sum_{n=1}^{n_*} \Big[4\tau\beta L(1 + \sqrt{Q_T})\|e_{n-1}^v\| + \tau\|R_n^x\|\Big].
$$

Then an application of the discrete Gronwall inequality yields

$$
\|e_{n_*}^x\| \le Q \sum_{n=1}^{n_*} \Big[\tau\|e_{n-1}^v\| + \tau\|R_n^x\|\Big].
$$

We incorporate this estimate with $\|R_n^x\| = O(\tau)$ to complete the proof.    □

Based on the derived results, we prove the error estimates of the explicit Euler scheme (3.3) in the following theorem.

THEOREM 3.4. *Suppose Assumption* A *holds. Then the following estimate holds:*

$$
\|e_n^x\| + \|e_n^v\| \le Q\tau, \quad 1 \le n \le N_T.
$$

*Here Q depends on L, T, and β but is independent of τ, n, and $N_T$.*

*Proof.* We subtract the second equation of (3.2) from that of (3.3) to obtain

$$
\begin{aligned}
v(t_n) - \tilde{v}_n &= e_{n-1}^v + \tau\gamma\big(J(x(t_{n-1}))v(t_{n-1}) - J(x_{n-1})v_{n-1}\big) \\
&\quad - \tau\gamma\big[v(t_{n-1})v(t_{n-1})^\top J(x(t_{n-1}))v(t_{n-1}) \\
&\quad\quad - v_{n-1}v_{n-1}^\top J(x_{n-1})v_{n-1}\big] + \tau R_n^v \\
&= e_{n-1}^v + \tau\gamma\big[(J(x(t_{n-1})) - J(x_{n-1}))v(t_{n-1}) + J(x_{n-1})e_{n-1}^v\big] \\
&\quad - \tau\gamma\big[e_{n-1}^v v(t_{n-1})^\top J(x(t_{n-1}))v(t_{n-1}) \\
&\quad\quad + v_{n-1}(e_{n-1}^v)^\top J(x(t_{n-1}))v(t_{n-1}) \\
&\quad\quad + v_{n-1}v_{n-1}^\top (J(x(t_{n-1})) - J(x_{n-1}))v(t_{n-1}) \\
&\quad\quad + v_{n-1}v_{n-1}^\top J(x_{n-1})e_{n-1}^v\big] + \tau R_n^v,
\end{aligned}
$$

which leads to

(3.14)
$$
\begin{aligned}
\|v(t_n) - \tilde{v}_n\| &\le \|e_{n-1}^v\| + \tau\gamma\big[L\|e_{n-1}^x\| + \bar{J}_T\|e_{n-1}^v\|\big] \\
&\quad + \tau\gamma\big[2J_T\|e_{n-1}^v\| + L\|e_{n-1}^x\| + \bar{J}_T\|e_{n-1}^v\|\big] + \tau R_n^v.
\end{aligned}
$$

We split $v(t_n) - \tilde{v}_n$ as $(v(t_n) - v_n) + (v_n - \tilde{v}_n) = e_n^v + (v_n - \tilde{v}_n)$ and apply Corollary 3.2 and Theorem 3.3 for (3.14) to get

(3.15)
$$
\begin{aligned}
\|e_n^v\| &\le \|e_{n-1}^v\| + \|v_n - \tilde{v}_n\| + Q\tau\big(\|e_{n-1}^x\| + \|e_{n-1}^v\|\big) + \tau\|R_n^v\| \\
&\le \|e_{n-1}^v\| + Q\tau\|e_{n-1}^v\| + Q\tau^2\sum_{m=1}^{n-1}\|e_m^v\| + Q\tau^2.
\end{aligned}
$$

Adding this equation from $n = 1$ to $n_*$ for $1 \le n_* \le N_T$ and using

$$
\tau^2\sum_{n=1}^{n_*}\sum_{m=1}^{n-1}\|e_m^v\| = \tau^2\sum_{m=1}^{n_*-1}\sum_{n=m+1}^{n_*}\|e_m^v\| \le T\tau\sum_{m=1}^{n_*-1}\|e_m^v\|
$$

we get

(3.16)
$$
\|e_{n_*}^v\| \le Q\tau\sum_{n=1}^{n_*-1}\|e_n^v\| + Q\tau.
$$

Then an application of the discrete Gronwall inequality leads to

$$
\|e_n^v\| \le Q\tau, \quad 1 \le n \le N_T.
$$

Plugging this estimate back to the conclusion of Theorem 3.3 yields the estimate of $\|e_n^x\|$ and we thus complete the proof. □

**4. Numerical analysis for index-$k$ saddle dynamics.** In this section, we consider the explicit Euler approximation of $k$-SD (2.1) for some $k > 1$ on the time interval $[0, T]$ for some $T > 0$ equipped with the initial conditions

(4.1)
$$
x(0) = x_0, \quad v_i(0) = v_{i,0} \text{ with } v_{i,0}^\top v_{j,0} = \delta_{i,j} \text{ for } 1 \le i, j \le k,
$$

where $\delta_{i,j} = 1$ if $i = j$ and $\delta_{i,j} = 0$ otherwise.

Compared with the 1-SD (2.3), which has only one eigenvector in the system and thus only requires the normalization at each time step, the $k$-SD has $k$ eigenvectors and thus needs an additional orthogonalization process, which significantly complicates the analysis.

**4.1. Explicit Euler scheme.** Similar to section 3.1, a reference equation for $k$-SD (2.1) reads

$$(4.2) \quad \begin{cases} x(t_n) = x(t_{n-1}) + \tau\beta\Big(I - 2\sum_{j=1}^{k} v_j(t_{n-1})v_j(t_{n-1})^\top\Big)F(x(t_{n-1})) + \tau R_n^x, \\[2mm] v_i(t_n) = v_i(t_{n-1}) + \tau\gamma\Big(I - v_i(t_{n-1})v_i(t_{n-1})^\top \\[2mm] \qquad\qquad -2\sum_{j=1}^{i-1} v_j(t_{n-1})v_j(t_{n-1})^\top\Big)J(x(t_{n-1}))v_i(t_{n-1}) + \tau R_n^{v_i}, \quad 1 \le i \le k. \end{cases}$$

Then we drop the truncation errors to obtain the explicit Euler scheme of (2.1) with the approximations $\{x_n, v_{i,n}\}_{n=1,i=1}^{N_T,k}$ to $\{x(t_n), v_i(t_n)\}_{n=1,i=1}^{N_T,k}$,

$$(4.3) \quad \begin{cases} x_n = x_{n-1} + \tau\beta\Big(I - 2\sum_{j=1}^{k} v_{j,n-1}v_{j,n-1}^\top\Big)F(x_{n-1}), \\[2mm] \tilde{v}_{i,n} = v_{i,n-1} + \tau\gamma\Big(I - v_{i,n-1}v_{i,n-1}^\top \\[2mm] \qquad\qquad -2\sum_{j=1}^{i-1} v_{j,n-1}v_{j,n-1}^\top\Big)J(x_{n-1})v_{i,n-1}, \quad 1 \le i \le k, \\[2mm] v_{i,n} = \frac{1}{Y_{i,n}}\Big(\tilde{v}_{i,n} - \sum_{j=1}^{i-1}(\tilde{v}_{i,n}^\top v_{j,n})v_{j,n}\Big), \quad 1 \le i \le k, \end{cases}$$

for $1 \le n \le N_T$ and

$$\begin{aligned} Y_{i,n} :&= \Big\|\tilde{v}_{i,n} - \sum_{j=1}^{i-1}(\tilde{v}_{i,n}^\top v_{j,n})v_{j,n}\Big\| \\ &= \Big(\|\tilde{v}_{i,n}\|^2 - 2\sum_{j=1}^{i-1}(\tilde{v}_{i,n}^\top v_{j,n})^2 + \sum_{j=1}^{i-1}(\tilde{v}_{i,n}^\top v_{j,n})v_{j,n}^\top \cdot \sum_{j=1}^{i-1}(\tilde{v}_{i,n}^\top v_{j,n})v_{j,n}\Big)^{1/2} \\ &= \Big(\|\tilde{v}_{i,n}\|^2 - \sum_{j=1}^{i-1}(\tilde{v}_{i,n}^\top v_{j,n})^2\Big)^{1/2}, \end{aligned}$$

equipped with the initial conditions (4.1). The third equation of (4.3) is indeed the Gram–Schmidt normalized orthogonalization procedure in order to preserve the orthonormal property of the vectors as in the continuous problem (2.1). Similar to the derivation of $\bar{J}_T$ in (3.4), we could conclude from the first equation of (4.3) that there exists a positive constant $\hat{J}_T$ independent of $N_T$ and $\tau$ such that $\max_{1 \le n \le N_T} \|J(x_n)\| \le \hat{J}_T$.

**4.2. Auxiliary estimates.** We prove several auxiliary estimates to support the error estimates. We will see that, compared with the numerical analysis of 1-SD, the orthogonality procedure in the Euler scheme (4.3) of $k$-SD brings additional difficulties that require subtle estimates.

LEMMA 4.1. *Under Assumption* A*, the following estimates hold for* $1 \le n \le N_T$:

$$\big|(\tilde{v}_{m,n})^\top \tilde{v}_{i,n}\big| \le M\tau^2, \quad 1 \le m < i \le k;$$

$$\big|\|\tilde{v}_{i,n}\| - 1\big| \le \big|\|\tilde{v}_{i,n}\|^2 - 1\big| \le M\tau^2, \quad 1 \le i \le k.$$

*Here the positive constant $M$ is independent of $n$, $N_T$, and $\tau$.*

*Proof.* To prove the first estimate, we directly calculate the product $\tilde{v}_{m,n}^\top \tilde{v}_{i,n}$ for $1 \le m < i \le k$,

(4.4)
$$
\tilde{v}_{m,n}^\top \tilde{v}_{i,n}
$$
$$
= \left[ v_{m,n-1} + \tau\gamma\left( I - v_{m,n-1}v_{m,n-1}^\top - 2\sum_{j=1}^{m-1} v_{j,n-1}v_{j,n-1}^\top \right) J(x_{n-1})v_{m,n-1} \right]^\top
$$
$$
\left[ v_{i,n-1} + \tau\gamma\left( I - v_{i,n-1}v_{i,n-1}^\top - 2\sum_{j=1}^{i-1} v_{j,n-1}v_{j,n-1}^\top \right) J(x_{n-1})v_{i,n-1} \right]
$$
$$
= \tau\gamma\left( v_{m,n-1}^\top J(x_{n-1})^\top v_{i,n-1} + v_{m,n-1}^\top J(x_{n-1})v_{i,n-1} - 2v_{m,n-1}^\top J(x_{n-1})v_{i,n-1} \right)
$$
$$
+ \tau^2\gamma^2\left[ \left( I - v_{m,n-1}v_{m,n-1}^\top - 2\sum_{j=1}^{m-1} v_{j,n-1}v_{j,n-1}^\top \right) J(x_{n-1})v_{m,n-1} \right]^\top
$$
$$
\left[ \left( I - v_{i,n-1}v_{i,n-1}^\top - 2\sum_{j=1}^{i-1} v_{j,n-1}v_{j,n-1}^\top \right) J(x_{n-1})v_{i,n-1} \right]
$$
$$
= \tau^2\gamma^2\left[ \left( I - v_{m,n-1}v_{m,n-1}^\top - 2\sum_{j=1}^{m-1} v_{j,n-1}v_{j,n-1}^\top \right) J(x_{n-1})v_{m,n-1} \right]^\top
$$
$$
\left[ \left( I - v_{i,n-1}v_{i,n-1}^\top - 2\sum_{j=1}^{i-1} v_{j,n-1}v_{j,n-1}^\top \right) J(x_{n-1})v_{i,n-1} \right],
$$

where we have used

$$
v_{m,n-1}^\top J(x_{n-1})^\top v_{i,n-1} + v_{m,n-1}^\top J(x_{n-1})v_{i,n-1} - 2v_{m,n-1}^\top J(x_{n-1})v_{i,n-1} = 0
$$

by the symmetry of $J$. Therefore, we apply the boundedness of $J$ to obtain for some constant $Q$

(4.5)
$$
\left| \tilde{v}_{m,n}^\top \tilde{v}_{i,n} \right| \le Q\tau^2, \quad 1 \le m < i \le k.
$$

We then turn to estimate the case $m = i$, that is, the norm $\|\tilde{v}_{i,n}\|^2$. By $\|v_{i,n-1}\| = 1$, we multiply $v_{i,n-1}^\top$ on both sides of the second equation of (4.3) to obtain for $1 \le i \le k$,

(4.6)
$$
v_{i,n-1}^\top \tilde{v}_{i,n} = v_{i,n-1}^\top v_{i,n-1} + \tau\gamma\left( v_{i,n-1}^\top - v_{i,n-1}^\top v_{i,n-1}v_{i,n-1}^\top \right.
$$
$$
\left. -2\sum_{j=1}^{i-1} v_{i,n-1}^\top v_{j,n-1}v_{j,n-1}^\top \right) J(x_{n-1})v_{i,n-1} = 1.
$$

We then multiply $\tilde{v}_{i,n}^\top$ on both sides of the second equation of (4.3) and apply (4.6) and the orthogonality of $\{v_{i,n-1}\}_{i=1}^k$ as well as

$$
\tilde{v}_{i,n}^\top v_{j,n-1} = (\tilde{v}_{i,n} - v_{i,n-1})^\top v_{j,n-1}, \quad 1 \le j < i,
$$

to obtain

$$
\begin{aligned}
\tilde{v}_{i,n}^\top \tilde{v}_{i,n} &= \tilde{v}_{i,n}^\top v_{i,n-1} + \tau\gamma\bigg(\tilde{v}_{i,n}^\top - \tilde{v}_{i,n}^\top v_{i,n-1} v_{i,n-1}^\top \\
&\qquad -2\sum_{j=1}^{i-1} \tilde{v}_{i,n}^\top v_{j,n-1} v_{j,n-1}^\top\bigg) J(x_{n-1}) v_{i,n-1} \\
&= 1 + \tau\gamma\bigg(\tilde{v}_{i,n}^\top - v_{i,n-1}^\top \\
&\qquad -2\sum_{j=1}^{i-1} (\tilde{v}_{i,n} - v_{i,n-1})^\top v_{j,n-1} v_{j,n-1}^\top\bigg) J(x_{n-1}) v_{i,n-1}.
\end{aligned}
\tag{4.7}
$$

Subtracting (4.6) from (4.7) and using $\big(\tilde{v}_{i,n} - v_{i,n-1}\big)^\top v_{i,n-1} = 0$ we get

$$
\begin{aligned}
\|\tilde{v}_{i,n} - v_{i,n-1}\|^2 &= \big(\tilde{v}_{i,n} - v_{i,n-1}\big)^\top \tilde{v}_{i,n} \\
&= \tau\gamma\bigg(\tilde{v}_{i,n}^\top - v_{i,n-1}^\top - 2\sum_{j=1}^{i-1} (\tilde{v}_{i,n} - v_{i,n-1})^\top v_{j,n-1} v_{j,n-1}^\top\bigg) J(x_{n-1}) v_{i,n-1} \\
&\leq \tau\gamma\hat{J}_T\big(1 + 2(i-1)\big)\|\tilde{v}_{i,n} - v_{i,n-1}\|,
\end{aligned}
$$

which gives

$$
\|\tilde{v}_{i,n} - v_{i,n-1}\| \leq \tau\gamma\hat{J}_T\big(1 + 2(i-1)\big).
$$

Invoking this in (4.7) leads to

$$
\begin{aligned}
\big|\|\tilde{v}_{i,n}\|^2 - 1\big| &\leq \tau\gamma\bigg(\|\tilde{v}_{i,n} - v_{i,n-1}\| + 2\sum_{j=1}^{i-1} \|\tilde{v}_{i,n} - v_{i,n-1}\|\bigg)\|J(x_{n-1})\| \\
&\leq \tau^2\big[\gamma\hat{J}_T\big(1 + 2(k-1)\big)\big]^2, \quad 1 \leq i \leq k, \quad 1 \leq n \leq N_T,
\end{aligned}
$$

which completes the proof.    □

LEMMA 4.2. *Under Assumption* A, *the following estimate holds for* $1 \leq n \leq N_T$ *and* $\tau$ *sufficiently small:*

$$
\|v_{i,n} - \tilde{v}_{i,n}\| \leq Q\tau^2, \quad 1 \leq i \leq k.
$$

*Here the positive constant* $Q$ *is independent of* $n$, $N_T$, *and* $\tau$.

*Proof.* We first estimate $\tilde{v}_{i,n}^\top v_{m,n}$ for $1 \leq m < i \leq k$ and $1 \leq n \leq N_T$. By the definition of $v_{m,n}$ in the third equation of (4.3), for a fixed $1 \leq m < k$ the estimates of $\tilde{v}_{i,n}^\top v_{m,n}$ for $m < i \leq k$ require those of $\tilde{v}_{i,n}^\top v_{j,n}$ for $1 \leq j < m$ and $m \leq i \leq k$. That is, we could estimate $\tilde{v}_{i,n}^\top v_{m,n}$ step by step with respect to $m$. There are various ways to perform the estimate with different constraints on $\tau$, and we present a simple choice for illustration.

Let $G > M$ be a fixed positive number where $M$ is defined in Lemma 4.1. Then we intend to prove that if $\tau$ satisfies the constraint

$$
\frac{M + \tau^2(k-1)G^2}{\big(1 - M\tau^2 - \tau^4(k-1)G^2\big)^{1/2}} \leq G,
\tag{4.8}
$$

then the following estimates hold:

$$(4.9) \qquad |\tilde{v}_{i,n}^{\top} v_{m,n}| \leq G\tau^2, \quad 1 \leq m < i \leq k.$$

Note that the condition (4.8) holds true if $\tau$ is sufficiently small. We prove this argument by induction on the subscription $m$. For $m = 1$ we apply Lemma 4.1 and the definition of $\tilde{v}_{1,n}$ in (4.3) as well as (4.8) to obtain

$$(4.10) \qquad \begin{aligned} |\tilde{v}_{i,n}^{\top} v_{1,n}| &= \frac{|\tilde{v}_{i,n}^{\top} \tilde{v}_{1,n}|}{(\|\tilde{v}_{1,n}\|^2)^{1/2}} \leq \frac{M\tau^2}{(1 - M\tau^2)^{1/2}} = \frac{M}{(1 - M\tau^2)^{1/2}}\tau^2 \\ &\leq \frac{M + \tau^2(k-1)G^2}{\left(1 - M\tau^2 - \tau^4(k-1)G^2\right)^{1/2}}\tau^2 \leq G\tau^2, \quad 1 < i \leq k. \end{aligned}$$

Thus, (4.9) holds with $m = 1$. Suppose (4.9) holds for $1 \leq m < m^*$ for some $1 \leq m^* < k - 1$. Then we invoke (4.9) with $1 \leq m < m^*$ and Lemma 4.1 into the expression of $\tilde{v}_{i,n}^{\top} v_{m^*,n}$ to obtain for $m^* < i \leq k$,

$$\begin{aligned} |\tilde{v}_{i,n}^{\top} v_{m^*,n}| &= \frac{\left| \tilde{v}_{i,n}^{\top} \tilde{v}_{m^*,n} - \sum_{j=1}^{m^*-1} (\tilde{v}_{m^*,n}^{\top} v_{j,n})(\tilde{v}_{i,n}^{\top} v_{j,n}) \right|}{\left( \|\tilde{v}_{m^*,n}\|^2 - \sum_{j=1}^{m^*-1} (\tilde{v}_{m^*,n}^{\top} v_{j,n})^2 \right)^{1/2}} \\ &\leq \frac{M\tau^2 + (m^*-1)(G\tau^2)^2}{(1 - M\tau^2 - (m^*-1)(G\tau^2)^2)^{1/2}} \\ &\leq \frac{M + \tau^2(k-1)G^2}{\left(1 - M\tau^2 - \tau^4(k-1)G^2\right)^{1/2}}\tau^2 \leq G\tau^2, \quad m^* < i \leq k. \end{aligned}$$

That is, (4.9) holds for $m = m^*$ and thus holds for any $1 \leq m < k$ by mathematical induction, which proves (4.9).

Based on (4.9) and Lemma 4.1, we bound $Y_{i,n}$ for $1 \leq i \leq k$ and $1 \leq n \leq N_T$ as follows:

$$(4.11) \qquad \begin{aligned} |Y_{i,n}| &= \left( \|\tilde{v}_{i,n}\|^2 - \sum_{j=1}^{i-1} (\tilde{v}_{i,n}^{\top} v_{j,n})^2 \right)^{1/2} \\ &\begin{cases} \leq \left( 1 + M\tau^2 + (i-1)G^2\tau^4 \right)^{1/2} \leq (1 + Q\tau^2)^{1/2}; \\ \geq \left( 1 - M\tau^2 - (i-1)G^2\tau^4 \right)^{1/2} \geq (1 - Q\tau^2)^{1/2} > 0. \end{cases} \end{aligned}$$

Then it remains to estimate $v_{i,n} - \tilde{v}_{i,n}$ for $1 \leq i \leq k$. According to the definition of $v_{i,n}$ we have

$$(4.12) \qquad v_{i,n} - \tilde{v}_{i,n} = \frac{1}{Y_{i,n}}\left( (1 - Y_{i,n})\tilde{v}_{i,n} - \sum_{j=1}^{i-1} (\tilde{v}_{i,n}^{\top} v_{j,n})v_{j,n} \right),$$

which, together with (4.9), (4.11), and Lemma 4.1, implies

$$
\begin{aligned}
\|v_{i,n} &- \tilde{v}_{i,n}\| \\
&\le \frac{1}{|Y_{i,n}|}\left(|1 - Y_{i,n}|\|\tilde{v}_{i,n}\| + \sum_{j=1}^{i-1}|\tilde{v}_{i,n}^{\top}v_{j,n}|\right) \\
&\le \frac{|1 - Y_{i,n}|(1 + M\tau^2) + (i-1)G\tau^2}{(1 - Q\tau^2)^{1/2}} \le Q|1 - Y_{i,n}| + Q\tau^2 \\
&\le Q\max\{1 - (1 - Q\tau^2)^{1/2}, (1 + Q\tau^2)^{1/2} - 1\} + Q\tau^2.
\end{aligned}
$$
(4.13)

We bound $1 - (1 - Q\tau^2)^{1/2}$ and $(1 + Q\tau^2)^{1/2} - 1$ by

$$
1 - (1 - Q\tau^2)^{1/2} = \frac{Q\tau^2}{1 + (1 - Q\tau^2)^{1/2}} \le Q\tau^2,
$$

$$
(1 + Q\tau^2)^{1/2} - 1 = \frac{Q\tau^2}{(1 + Q\tau^2)^{1/2} + 1} \le Q\tau^2.
$$

Thus we complete the proof.                                                □

**4.3. Error estimates.** Define the errors

$$
e_n^x := x(t_n) - x_n, \quad e_{i,n}^v := v_i(t_n) - v_{i,n}, \quad 1 \le n \le N_T, \quad 1 \le i \le k.
$$

We then perform the error estimates for the explicit Euler scheme (4.3) of $k$-SD (2.1) in the following theorem.

THEOREM 4.3. *Suppose Assumption* A *holds. Then the following estimate holds for $\tau$ sufficiently small:*

$$
\|e_n^x\| + \sum_{i=1}^{k}\|e_{i,n}^v\| \le Q\tau, \quad 1 \le n \le N_T.
$$

*Here $Q$ depends on $k$, $L$, $T$, and $\beta$ but is independent of $\tau$, $n$, and $N_T$.*

*Proof.* Similar to the derivations in Theorem 3.3 we could bound $e_n^x$ in terms of $e_{i,n}^v$ for $1 \le i \le k$ as follows:

$$
\|e_n^x\| \le Q\tau\sum_{m=1}^{n-1}\sum_{j=1}^{k}\|e_{j,m}^v\| + Q\tau, \quad 1 \le n \le N_T.
$$
(4.14)

We subtract the second equation of (4.2) from that of (4.3) and apply $v_i(t_n) - \tilde{v}_{i,n}$ as $(v_i(t_n) - v_{i,n}) + (v_{i,n} - \tilde{v}_{i,n}) = e_{i,n}^v + (v_{i,n} - \tilde{v}_{i,n})$ to obtain

$$
\begin{aligned}
e_{i,n}^v = {}& e_{i,n-1}^v + \tau\gamma\big(J(x(t_{n-1}))v_i(t_{n-1}) - J(x_{n-1})v_{i,n-1}\big) \\
&- \tau\gamma\big[v_i(t_{n-1})v_i(t_{n-1})^{\top}J(x(t_{n-1}))v_i(t_{n-1}) \\
&\quad - v_{i,n-1}v_{i,n-1}^{\top}J(x_{n-1})v_{i,n-1}\big] \\
&- 2\tau\gamma\sum_{j=1}^{i-1}\big[v_j(t_{n-1})v_j(t_{n-1})^{\top}J(x(t_{n-1}))v_i(t_{n-1}) \\
&\quad - v_{j,n-1}v_{j,n-1}^{\top}J(x_{n-1})v_{i,n-1}\big] - (v_{i,n} - \tilde{v}_{i,n}) + \tau R_n^{v_i},
\end{aligned}
$$

which, together with (4.14), Lemma 4.2, and the similar derivation as (3.14), leads to

$$\|e_{i,n}^v\| \le \|e_{i,n-1}^v\| + Q\tau\big[\|e_{n-1}^x\| + \|e_{i,n-1}^v\|\big] + Q\tau \sum_{j=1}^{i-1} \|e_{j,n-1}^v\| + Q\tau^2$$

$$\le \|e_{i,n-1}^v\| + Q\tau\|e_{i,n-1}^v\| + Q\tau^2 \sum_{m=1}^{n-1}\sum_{j=1}^{k} \|e_{j,m}^v\| + Q\tau \sum_{j=1}^{i-1} \|e_{j,n-1}^v\| + Q\tau^2.$$

Adding this equation from $i = 1$ to $k$ and denoting

$$E_n^v := \sum_{i=1}^{k} \|e_{i,n}^v\|, \quad 1 \le n \le N_T,$$

yield an estimate in terms of $E_n^v$

$$(4.15) \qquad E_n^v \le E_{n-1}^v + Q\tau E_{n-1}^v + Q\tau^2 \sum_{m=1}^{n-1} E_m^v + Q\tau^2.$$

Adding this equation from $n = 1$ to $n_*$ and using

$$\tau^2 \sum_{n=1}^{n_*}\sum_{m=1}^{n-1} E_m^v = \tau^2 \sum_{m=1}^{n_*-1}\sum_{n=m+1}^{n_*} E_m^v \le T\tau \sum_{m=1}^{n_*-1} E_m^v,$$

we get

$$(4.16) \qquad E_{n_*}^v \le Q\tau \sum_{n=1}^{n_*-1} E_n^v + Q\tau.$$

Then an application of the discrete Gronwall inequality leads to

$$E_n^v \le Q\tau, \quad 1 \le n \le N_T.$$

Plugging this estimate back to (4.14) yields the estimate of $\|e_n^x\|$ and we thus complete the proof. $\qquad\square$

**5. Numerical experiments.** In this section, we carry out numerical experiments to substantiate the accuracy of the explicit Euler schemes (3.3) and (4.3) and the pathway convergence of the numerical solutions to the real searching pathway of HiSD. For the applications of these schemes, we refer the reader to [30, 31] for various physical examples and detailed discussions. We denote the following errors:

$$\begin{aligned}
\mathrm{Err}(x) &:= \max_{1 \le n \le N_T} \|x(t_n) - x_n\|, \\
\mathrm{Err}(v) &:= \max_{1 \le n \le N_T} \|v(t_n) - v_n\|, \\
\mathrm{Err}(v_i) &:= \max_{1 \le n \le N_T} \|v_i(t_n) - v_{i,n}\|, \quad 1 \le i \le k,
\end{aligned}$$

and test their convergence rates. As the exact solutions to HiSD are not available, numerical solutions computed under $\tau = 2^{-13}$ serve as the reference solutions for the first two examples, and we set $\beta = \gamma = T = 1$ for simplicity.

**Example 1. Accuracy test under Minyaev–Quapp surface.** We consider the saddle dynamics for the Minyaev–Quapp surface (2.4) and compute its index-1

saddle point via scheme (3.3) with the initial conditions $x(0) = (1, 1)^\top$ and $v(0) = (0, 1)^\top$ and index-2 saddle point via scheme (4.3) with the initial conditions $x(0) = (1, 1)^\top$, $v_1(0) = (0, 1)^\top$, and $v_2(0) = (1, 0)^\top$. Numerical results are presented in Tables 5.1–5.2, which demonstrate the first-order accuracy of the explicit Euler schemes (3.3) and (4.3) as proved in Theorems 3.4 and 4.3.

TABLE 5.1
*Convergence rates of scheme* (3.3) *in Example* 1.

| $\tau$ | Err$(x)$ | Conv. rate | Err$(v)$ | Conv. rate |
|---|---|---|---|---|
| 1/32 | 2.19E-02 | | 1.72E-02 | |
| 1/64 | 1.03E-02 | 1.09 | 8.29E-03 | 1.05 |
| 1/128 | 4.95E-03 | 1.05 | 4.05E-03 | 1.03 |
| 1/256 | 2.40E-03 | 1.04 | 1.98E-03 | 1.03 |

TABLE 5.2
*Convergence rates of scheme* (4.3) *in Example* 1.

| $\tau$ | Err$(x)$ | Conv. rate | Err$(v_1)$ | Conv. rate | Err$(v_2)$ | Conv. rate |
|---|---|---|---|---|---|---|
| 1/32 | 1.50E-02 | | 1.31E-02 | | 1.31E-02 | |
| 1/64 | 7.41E-03 | 1.02 | 6.52E-03 | 1.01 | 6.52E-03 | 1.01 |
| 1/128 | 3.66E-03 | 1.02 | 3.23E-03 | 1.01 | 3.23E-03 | 1.01 |
| 1/256 | 1.79E-03 | 1.03 | 1.59E-03 | 1.02 | 1.59E-03 | 1.02 |

**Example 2: Accuracy test under Eckhardt surface.** We consider the saddle dynamics for the Eckhardt surface (2.5) and compute its index-1 saddle point via scheme (3.3) with the initial conditions

$$x(0) = (-2, 1)^\top, \quad v(0) = \frac{1}{\sqrt{2}}(-1, 1)^\top$$

and index-2 saddle point via scheme (4.3) with the initial conditions

$$x(0) = (-2, 1)^\top, \quad v_1(0) = \frac{1}{\sqrt{10}}(-1, 3)^\top, \quad v_2(0) = \frac{1}{\sqrt{10}}(3, 1)^\top.$$

Numerical results are presented in Tables 5.3–5.4, which again show the first-order accuracy of the explicit Euler schemes (3.3) and (4.3) as proved in Theorems 3.4 and 4.3.

TABLE 5.3
*Convergence rates of scheme* (3.3) *in Example* 2.

| $\tau$ | Err$(x)$ | Conv. rate | Err$(v)$ | Conv. rate |
|---|---|---|---|---|
| 1/32 | 1.41E-02 | | 2.16E-03 | |
| 1/64 | 6.98E-03 | 1.01 | 1.09E-03 | 0.98 |
| 1/128 | 3.45E-03 | 1.01 | 5.46E-04 | 1.00 |
| 1/256 | 1.70E-03 | 1.02 | 2.70E-04 | 1.02 |

TABLE 5.4
*Convergence rates of scheme* (4.3) *in Example* 2.

| $\tau$ | Err$(x)$ | Conv. rate | Err$(v_1)$ | Conv. rate | Err$(v_2)$ | Conv. rate |
|---|---|---|---|---|---|---|
| 1/32 | 5.78E-03 | | 2.25E-03 | | 2.25E-03 | |
| 1/64 | 2.86E-03 | 1.02 | 1.11E-03 | 1.01 | 1.11E-03 | 1.01 |
| 1/128 | 1.41E-03 | 1.02 | 5.51E-04 | 1.02 | 5.51E-04 | 1.02 |
| 1/256 | 6.95E-04 | 1.03 | 2.71E-04 | 1.03 | 2.71E-04 | 1.03 |

**Example 3: Convergence of dynamics under Eckhardt surface.** In this example we aim to observe the numerical convergence of dynamics for HiSD. As the exact dynamics of HiSD is not available in practice, we approximate it by the numerical solutions under the very fine mesh size $\tau = 2^{-8}$. The initial conditions are given as

$$x(0) = (1.5, 1.2)^\top, \quad v(0) = \frac{1}{\sqrt{5}}(-1, 2)^\top.$$

Figure 5.1 (left) indicates that the HiSD reaches a saddle point under both $T = 10$ and $T = 5$ and thus it suffices to take $T = 5$. Figure 5.1 (right) shows that not only can the saddle point be achieved under different step sizes, but the dynamics of HiSD globally converges to the exact one (i.e., the curve under $\tau = 2^{-8}$) as the step size $\tau$ decreases. These observations justify the theoretical results and demonstrate that the proposed schemes are appropriate methods in computing the dynamic pathways for constructing the solution landscapes, e.g., [14, 26, 30].
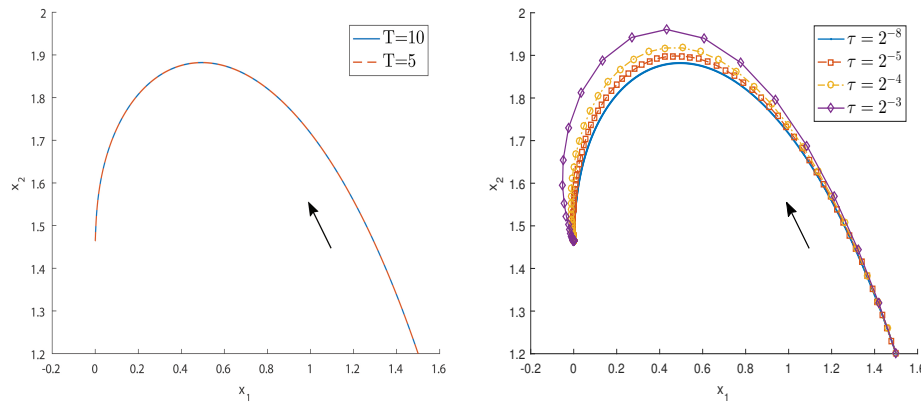


FIG. 5.1. *(Left) Numerical solution of $x(t)$ with $\tau = 2^{-8}$ and different terminal time $T$. (Right) Numerical solution of $x(t)$ with $T = 5$ and different $\tau$. The symbols on the curves indicate the time steps.*

**6. Extension to generalized HiSD for dynamical systems.** In many autonomous dynamical systems $\dot{x} = F(x)$, the force $F(x)$ is not derived from the variation of some energy function/functional $E(x)$, which does not follow the formulations of the HiSD proposed in section 2. In this case, the following GHiSD was developed in [30] to compute the high-index saddle points for nongradient systems:

$$(6.1) \quad \begin{cases} \dfrac{dx}{dt} = \left(I - 2\sum_{j=1}^{k} v_j v_j^\top\right) F(x), \\ \dfrac{dv_i}{dt} = (I - v_i v_i^\top)\tilde{J}(x)v_i - \sum_{j=1}^{i-1} v_j v_j^\top(\tilde{J}(x) + \tilde{J}^\top(x))v_i, \quad 1 \leq i \leq k. \end{cases}$$

Here $\tilde{J}$ refers to the Jacobian of $F$, which is, in general, not symmetric. Compared with the HiSD (2.1), which works for the gradient systems with the symmetric Hessian $J(x)$, $\tilde{J}(x) + \tilde{J}^\top(x)$ is used to replace $2J(x)$ in the dynamics of $\{v_i\}_{i=1}^{k}$.

Similar to (4.3), we could propose the explicit Euler scheme of (6.1) for $1 \leq n \leq$

$N_T$ as follows:

$$
(6.2) \quad
\begin{cases}
x_n = x_{n-1} + \tau \left( I - 2 \sum_{j=1}^{k} v_{j,n-1} v_{j,n-1}^\top \right) F(x_{n-1}), \\[2mm]
\tilde{v}_{i,n} = v_{i,n-1} + \tau \left( I - v_{i,n-1} v_{i,n-1}^\top \right) \tilde{J}(x_{n-1}) v_{i,n-1} \\[2mm]
\qquad\qquad - \sum_{j=1}^{i-1} v_{j,n-1} v_{j,n-1}^\top \left( \tilde{J}(x_{n-1}) + \tilde{J}^\top(x_{n-1}) \right) v_{i,n-1}, \quad 1 \le i \le k, \\[2mm]
v_{i,n} = \dfrac{1}{Y_{i,n}} \left( \tilde{v}_{i,n} - \sum_{j=1}^{i-1} (\tilde{v}_{i,n}^\top v_{j,n}) v_{j,n} \right), \quad 1 \le i \le k.
\end{cases}
$$

Intuitively, we may extend the developed methods and results in previous sections to GHiSD (6.1) for nongradient systems. Although there are differences between (2.1) and (6.1) as mentioned above, we notice that the derivations could be performed similarly. After carefully checking the preceding estimates, a key step lies in the quantification of $\tilde{v}_{m,n}^\top \tilde{v}_{i,n}$ in (4.4). We thus calculate this product for $m < i$ for the case of generalized saddle dynamics (6.1) as follows:

$$
\begin{aligned}
\tilde{v}_{m,n}^\top \tilde{v}_{i,n} &= \Big[ v_{m,n-1} + \tau \big( I - v_{m,n-1} v_{m,n-1}^\top \big) \tilde{J}(x_{n-1}) v_{m,n-1} \\
&\qquad - \tau \sum_{j=1}^{m-1} v_{j,n-1} v_{j,n-1}^\top \big( \tilde{J}(x_{n-1}) + \tilde{J}^\top(x_{n-1}) \big) v_{m,n-1} \Big]^\top \\
&\quad \Big[ v_{i,n-1} + \tau \big( I - v_{i,n-1} v_{i,n-1}^\top \big) \tilde{J}(x_{n-1}) v_{i,n-1} \\
&\qquad - \sum_{j=1}^{i-1} v_{j,n-1} v_{j,n-1}^\top \big( \tilde{J}(x_{n-1}) + \tilde{J}^\top(x_{n-1}) \big) v_{i,n-1} \Big] \\
&= \tau \big( v_{m,n-1}^\top \tilde{J}(x_{n-1}) v_{i,n-1} + v_{m,n-1}^\top \tilde{J}^\top(x_{n-1}) v_{i,n-1} \\
&\qquad - v_{m,n-1}^\top \big( \tilde{J}(x_{n-1}) + \tilde{J}^\top(x_{n-1}) \big) v_{i,n-1} \big) + \tau^2[\cdots] = \tau^2[\cdots],
\end{aligned}
$$

where we used the fact that

$$
\begin{aligned}
v_{m,n-1}^\top \tilde{J}(x_{n-1}) v_{i,n-1} + v_{m,n-1}^\top \tilde{J}^\top(x_{n-1}) v_{i,n-1} \\
- v_{m,n-1}^\top \big( \tilde{J}(x_{n-1}) + \tilde{J}^\top(x_{n-1}) \big) v_{i,n-1} = 0.
\end{aligned}
$$

Note that this nice property stems from the symmetrization $\tilde{J}(x) + \tilde{J}^\top(x)$ in the GHiSD (6.1). By virtue of this symmetrization, we could derive the error estimates for explicit Euler scheme (6.2) in parallel with the proofs in previous sections, and thus show the numerical accuracy of GHiSD (6.1) for nongradient systems.

**7. Conclusions.** In this paper we develop novel techniques to overcome the strong nonlinearity and the difficulties caused by the orthonormalization procedure to prove error estimates for Euler discretization of HiSD with respect to the time step size, which serves as an important compensation for the gap between the continuous problem and the numerical implementation. The developed methods and results are further extended to study the GHiSD for nongradient systems, and thus provide theoretical supports for the accuracy of numerical computations.

There are several other potential extensions of the current work. For instance, the ideas and techniques could be employed and improved to analyze implicit schemes or high-order methods like the backward difference formulas of HiSD in order to retain high-order accuracy. How to relax the linear growth and Lipschitz conditions on the force $F$ and the Hessian $J$ (or Jacobian in nongradient systems) in the error estimates is also an important but challenging topic as many energy surfaces do not enjoy these properties. We may further extend the methods to study the numerical schemes of the dimer-type methods such as the shrinking dimer dynamics [33]. However, as the multiplication of the Hessian and the vector is approximated by dimer methods in order to reduce the computational costs, the current Hessian-based proofs do not apply, and additional investigations will be carried out in the near future. Recently, a constrained high-index saddle dynamics (CHiSD) was developed to compute high-index saddle points of an energy functional subject to equality constraints [27]. Applying the Riemannian gradients and Hessians, the CHiSD is derived as the dynamical system with a transformed gradient flow. In the numerical implementation, the retraction operator and vector transport are introduced to discretize the CHiSD. Thus, it will be very interesting to study the error estimates for numerical schemes of CHiSD in the future.

It is also worth mentioning that in the current work we focus on the dynamics of HiSD on the finite interval $t \in [0, T]$ and prove error estimates to show the pathway convergence of numerical solutions of HiSD. For most applications, numerical schemes of HiSD could reach the target saddle point within a certain number of iterations (e.g., the observations in the left plot of Figure 5.1), and thus the derived error estimate results in this work could apply by setting a suitable $T$. Nevertheless, the convergence to the saddle point is theoretically determined by the rate of $x(t) \to x_*$ as $t \to \infty$; thus it is desirable to perform the error estimate of $x_n - x_*$ for $n \to \infty$ as in the literature of optimization algorithms [17, 23]. In a very recent work [19] the convergence analysis of HiSD is performed to determine the convergence rate of $x_n - x_*$ for $n \to \infty$. It should be pointed out that the result in the current work that $v_{1,n} - v_1(t_n)$ has the first-order accuracy with respect to the time step size was borrowed in [19] in order to prove the approximation of eigenvector, which again shows the importance of novel techniques proposed in this work.

## REFERENCES

[1] J. Baker, *An algorithm for the location of transition states*, J. Comput. Chem., 7 (1986), pp. 385–395.

[2] H. Brunner, *Collocation Methods for Volterra Integral and Related Functional Differential Equations*, Cambridge University Press, Cambridge, UK, 2004.

[3] J. Doye and D. Wales, *Saddle points and dynamics of Lennard-Jones clusters, solids, and supercooled liquids*, J. Chem. Phys., 116 (2002), pp. 3777–3788.

[4] B. Eckhardt, *Irregular scattering*, Phys. D, 33 (1988), pp. 89–98.

[5] W. E and E. Vanden-Eijnden, *Transition-path theory and path-finding algorithms for the study of rare events*, Annu. Rev. Phys. Chem., 61 (2010), pp. 391–420.

[6] W. E and X. Zhou, *The gentlest ascent dynamics*, Nonlinearity, 24 (2011), pp. 1831–1842.

[7] P. E. Farrell, Á. Birkisson, and S. W. Funke, *Deflation techniques for finding distinct solutions of nonlinear partial differential equations*, SIAM J. Sci. Comput., 37 (2015), pp. A2026–A2045, https://doi.org/10.1137/140984798.

[8] W. Gao, J. Leng, and X. Zhou, *An iterative minimization formulation for saddle point search*, SIAM J. Numer. Anal., 53 (2015), pp. 1786–1805, https://doi.org/10.1137/130930339.

[9] I. Goodfellow, Y. Bengio, and A. Courville, *Deep Learning*, MIT Press, Cambridge, MA, 2016.

[10] N. Gould, C. Ortner, and D. Packwood, *A dimer-type saddle search algorithm with pre-*

*conditioning and linesearch*, Math. Comp., 85 (2016), pp. 2939–2966.

[11] Y. Han, Y. Hu, P. Zhang, A. Majumdar, and L. Zhang, *Transition pathways between defect patterns in confined nematic liquid crystals*, J. Comput. Phys., 396 (2019), pp. 1–11.

[12] Y. Han, Z. Xu, A. Shi, and L. Zhang, *Pathways connecting two opposed bilayers with a fusion pore: A molecularly-informed phase field approach*, Soft Matter, 16 (2020), pp. 366–374.

[13] Y. Han, J. Yin, Y. Hu, A. Majumdar, and L. Zhang, *Solution landscapes of the simplified Ericksen-Leslie model and its comparison with the reduced Landau-de Gennes model*, Proc. A, 477 (2021), 20210458.

[14] Y. Han, J. Yin, P. Zhang, A. Majumdar, and L. Zhang, *Solution landscape of a reduced Landau–de Gennes model on a hexagon*, Nonlinearity, 34 (2021), pp. 2048–2069.

[15] G. Henkelman and H. Jónsson, *A dimer method for finding saddle points on high dimensional potential surfaces using only first derivatives*, J. Chem. Phys., 111 (1999), pp. 7010–7022.

[16] A. Levitt and C. Ortner, *Convergence and cycling in Walker-type saddle search algorithms*, SIAM J. Numer. Anal., 55 (2017), pp. 2204–2227, https://doi.org/10.1137/16M1087199.

[17] C. Li, M. Wang, H. Liu, and T. Zhang, *Near-optimal stochastic approximation for online principal component estimation*, Math. Program., 167 (2018), pp. 75–97.

[18] Y. Li and J. Zhou, *A minimax method for finding multiple critical points and its applications to semilinear PDEs*, SIAM J. Sci. Comput., 23 (2001), pp. 840–865, https://doi.org/10.1137/S1064827599365641.

[19] Y. Luo, X. Zheng, X. Cheng, and L. Zhang, *Convergence Analysis of Discrete High-index Saddle Dynamics*, preprint, https://arxiv.org/abs/2204.00171, 2022.

[20] D. Mehta, *Finding all the stationary points of a potential-energy landscape via numerical polynomial-homotopy-continuation method*, Phys. Rev. E, 84 (2011), 025702.

[21] J. W. Milnor, *Morse Theory*, Princeton University Press, Princeton, NJ, 1963.

[22] R. M. Minyaev, W. Quapp, G. Subramanian, P. R. Schleyer, and Y. Ho, *Internal conrotation and disrotation in $H_2BCH_2BH_2$ and diborylmethane $1, 3\,H$ exchange*, J. Comput. Chem., 18 (1997), pp. 1792–1803.

[23] Y. Nesterov, *Introductory Lectures on Convex Optimization: A Basic Course*, Appl. Optim. 87, Kluwer Academic Publishers, Boston, 2004.

[24] W. Wang, L. Zhang, and P. Zhang, *Modelling and computation of liquid crystals*, Acta Numer., 30 (2021), pp. 765–851.

[25] X. Xu, C. L. Ting, I. Kusaka, and Z. G. Wang, *Nucleation in polymers and soft matter*, Annu. Rev. Phys. Chem., 65 (2014), pp. 449–475.

[26] Z. Xu, Y. Han, J. Yin, B. Yu, Y. Nishiura, and L. Zhang, *Solution landscapes of the diblock copolymer-homopolymer model under two-dimensional confinement*, Phys. Rev. E, 104 (2021), 014505.

[27] J. Yin, Z. Huang, and L. Zhang, *Constrained high-index saddle dynamics for the solution landscape with equality constraints*, J. Sci. Comput., 91 (2022), 62.

[28] J. Yin, K. Jiang, A.-C. Shi, P. Zhang, and L. Zhang, *Transition pathways connecting crystals and quasicrystals*, Proc. Natl. Acad. Sci. USA, 118 (2021), e2106230118.

[29] J. Yin, Y. Wang, J. Chen, P. Zhang, and L. Zhang, *Construction of a pathway map on a complicated energy landscape*, Phys. Rev. Lett., 124 (2020), 090601.

[30] J. Yin, B. Yu, and L. Zhang, *Searching the solution landscape by generalized high-index saddle dynamics*, Sci. China Math., 64 (2021), pp. 1801–1816.

[31] J. Yin, L. Zhang, and P. Zhang, *High-index optimization-based shrinking dimer method for finding high-index saddle points*, SIAM J. Sci. Comput., 41 (2019), A3576–A3595, https://doi.org/10.1137/19M1253356.

[32] J. Yin, L. Zhang, and P. Zhang, *Solution landscape of Onsager functional identifies non-axisymmetric critical points*, Phys. D, 430 (2022), 133081.

[33] J. Zhang and Q. Du, *Shrinking dimer dynamics and its applications to saddle point search*, SIAM J. Numer. Anal., 50 (2012), pp. 1899–1921, https://doi.org/10.1137/110843149.

[34] L. Zhang, L. Chen, and Q. Du, *Morphology of critical nuclei in solid-state phase transformations*, Phys. Rev. Lett., 98 (2007), 265703.

[35] L. Zhang, L. Chen, and Q. Du, *Simultaneous prediction of morphologies of a critical nucleus and an equilibrium precipitate in solids*, Commun. Comput. Phys., 7 (2010), pp. 674–682.

[36] L. Zhang, Q. Du, and Z. Zheng, *Optimization-based shrinking dimer method for finding transition states*, SIAM J. Sci. Comput., 38 (2016), pp. A528–A544, https://doi.org/10.1137/140972676.

[37] L. Zhang, W. Ren, A. Samanta, and Q. Du, *Recent developments in computational modelling of nucleation in phase transformations*, npj Comput. Mater., 2 (2016), 16003.